



**HAL**  
open science

## Global importance of oxic molybdenum sinks prior to 2.6 Ga revealed by the Mo isotope composition of Precambrian carbonates

Marie Thoby, Kurt O. Konhauser, Philip Fralick, Wladyslaw Altermann, Pieter T. Visscher, Stefan Lalonde

### ► To cite this version:

Marie Thoby, Kurt O. Konhauser, Philip Fralick, Wladyslaw Altermann, Pieter T. Visscher, et al.. Global importance of oxic molybdenum sinks prior to 2.6 Ga revealed by the Mo isotope composition of Precambrian carbonates. *Geology*, 2019, 47 (6), pp.559-562. 10.1130/g45706.1 . hal-02300734

**HAL Id: hal-02300734**

**<https://hal.univ-brest.fr/hal-02300734>**

Submitted on 29 Sep 2019

**HAL** is a multi-disciplinary open access archive for the deposit and dissemination of scientific research documents, whether they are published or not. The documents may come from teaching and research institutions in France or abroad, or from public or private research centers.

L'archive ouverte pluridisciplinaire **HAL**, est destinée au dépôt et à la diffusion de documents scientifiques de niveau recherche, publiés ou non, émanant des établissements d'enseignement et de recherche français ou étrangers, des laboratoires publics ou privés.

1

2 Global importance of oxic molybdenum sinks prior to 2.6  
3 Ga revealed by the Mo isotope composition of Precambrian  
4 carbonates

5 Marie Thoby<sup>1</sup>, Kurt O. Konhauser<sup>2</sup>, Philip W. Fralick<sup>3</sup>, Wladyslaw Altermann<sup>4</sup>,  
6 Pieter T. Visscher<sup>5</sup>, and Stefan V. Lalonde<sup>1</sup>

7 <sup>1</sup>*CNRS-UMR6538 Laboratoire Géosciences Océan, Institut Universitaire Européen de la*  
8 *Mer, Université de Bretagne Occidentale, Brest, France*

9 <sup>2</sup>*Department of Earth and Atmospheric Sciences, University of Alberta, Edmonton,*  
10 *Alberta T6G 2E3, Canada*

11 <sup>3</sup>*Department of Geology, Lakehead University, Thunder Bay, Ontario P7B 5E1, Canada*

12 <sup>4</sup>*Department of Geology, University of Pretoria, Private bag X20, Hatfield, Pretoria*  
13 *0028, South Africa*

14 <sup>5</sup>*Department of Marine Sciences, University of Connecticut, Groton, Connecticut 06340,*  
15 *USA*

16

17 **ABSTRACT**

18       Sedimentary molybdenum (Mo) isotope compositions are a promising paleoredox  
19 indicator as the Mo isotope composition of seawater reflects the balance between anoxic  
20 and oxic sinks. Most available data are from shales, however the Mo isotope composition  
21 of carbonates also reflects the composition of ancient seawater. Here we provide an  
22 expanded dataset of carbonate Mo isotope compositions, including the first data for  
23 carbonates older than 2.64 Ga, which we evaluate against a compilation of published data  
24 for carbonates, shales, and iron formations spanning geological time. Archean carbonate  
25 samples reveal maximum  $\delta^{98}\text{Mo}$  values that are generally above 1‰. These heavy values  
26 indicate that Mn(IV)- or Fe(III)-oxide sinks were sufficiently important to influence the  
27 Mo isotope composition of seawater as far back as 2.93 Ga. Comparison of Mo isotope  
28 and rare earth element data, as well as residence time considerations, indicates that this  
29 metal oxide influence was likely global. Available Mo isotope data for shales over the  
30 same time period generally show crustal values, which we attribute to negligible  
31 authigenic enrichment of Mo from seawater due to low ambient concentrations and a  
32 paucity of euxinic conditions. Our work demonstrates that the carbonate record provides  
33 important new insights into marine paleoredox, especially when shale records are absent  
34 or unsuitable, and re-enforces the emerging paradigm that oxic Mo sinks were important  
35 in the marine realm prior to 2.7 Ga.

36

37 **INTRODUCTION**

38 Molybdenum (Mo) stable isotopes have emerged as a powerful proxy for marine  
39 redox evolution that is based on the redox sensitive nature of Mo sources and sinks.  
40 Under modern oxic conditions, seawater shows a homogenous value of 2.36‰ (Siebert et  
41 al., 2003; Figure DR1 in the GSA Data Repository<sup>1</sup>). Modern Mo seawater sources are  
42 principally derived from the oxidative weathering of continental crust sulfide minerals  
43 (~90%; mean  $\delta^{98}\text{Mo}$  value of 0.20‰; Siebert et al., 2003; Voegelin et al., 2012) variably  
44 modified during transport to values as high as 2.39‰ (e.g., Voegelin et al., 2012).  
45 Modern Mo sinks are dominated by Mn(IV) and Fe(III) oxide minerals that sequester Mo  
46 by adsorption and co-precipitation. With an equilibrium Mo fractionation of 3.3‰ onto  
47 Mn(IV) oxides (Siebert et al., 2003, Barling and Anbar, 2004) and from 0.83 to 2.19‰  
48 onto Fe(III) oxides (Goldberg et al. 2009), they constitute the isotopically lightest sink  
49 and are responsible for the heavy Mo isotope enrichment of seawater. The second most  
50 important sink is sedimentary Mo scavenging under suboxic, anoxic, and euxinic  
51 conditions, which also favor the lighter isotope but to a lesser degree (see Figure DR1).  
52 As sulfide increases, sediment isotope compositions approach that of seawater as Mo  
53 scavenging becomes near-quantitative (e.g., Neubert et al., 2008). This explains why  
54 black shales are used to track marine paleoredox using Mo isotopes.

55 The Mo isotope proxy has been used to provide critical insights into the relative  
56 importance of oxic and anoxic marine waters through geological time. Arnold et al.  
57 (2004) reported  $\delta^{98}\text{Mo}$  values ~-0.69‰ for mid-Proterozoic euxinic sediments of the  
58 Velkerri (1.40 Ga) and Wollogorang (1.70 Ga) formations, implying significant areas of  
59 seafloor anoxia at the time. Heavy Mo isotope signatures in shales extend back to 2.60

60 Ga. Conversely, prior to 2.60 Ga, shales generally show crustal Mo isotope values  
61 (Siebert et al., 2005; Wille et al., 2007), suggesting that either oxic Mo sinks were  
62 minimal prior to the Great Oxygenation Event (GOE) ca. 2.45 Ga, or that Mo in shales is  
63 a poor proxy for Archean oxygenation. Interestingly, Planavsky et al. (2014)  
64 demonstrated that iron formation (IF) as old as 2.95 Ga show highly fractionated  $\delta^{98}\text{Mo}$   
65 values ranging from -0.71‰ to 2.32‰, which vary as a function of Fe/Mn ratio. The  
66 lightest values are best explained by syndepositional adsorption of Mo to Mn(IV) oxides,  
67 implying that sufficient  $\text{O}_2$  for Mn(II) oxidation, and thus the evolution of oxidative  
68 photosynthesis, had already occurred by 2.95 Ga.

69 Here we turn here to another sedimentary proxy capable of recording ancient Mo  
70 cycling: the molybdenum isotope composition of Mo hosted in carbonates ( $\delta^{98}\text{Mo}_{\text{carb}}$ ;  
71 Voegelin et al., 2009; 2010; Wen et al., 2011; Eroglu et al., 2015; Romaniello et al.,  
72 2016). Although carbonates are a negligible Mo sink, they may record the  $\delta^{98}\text{Mo}$   
73 signature of seawater from which they were formed (Voegelin et al., 2009; Romaniello et  
74 al., 2016). Our study provides an expanded dataset for modern and Archean carbonate  
75 Mo isotopic compositions, which we compare to published data from carbonate, shale,  
76 and iron formation records to shed new light on marine Mo cycling in the Archean.

77

78 **SAMPLES AND METHODS**

79       The newly acquired Mo isotopic data presented here include modern thrombolites  
80 and stromatolites from the Bahamas, 2.52 Ga stromatolites from the Gamohaan  
81 Formation (Ghaap Group, S. Africa), crystal fans and stromatolites from the 2.80 Ga  
82 Mosher Carbonate (Steep Rock Group, Canada) and 2.93 Ga Ball Assemblage (Red Lake  
83 Greenstone Belt, Canada), and 2.97 Ga stromatolitic and non-stromatolitic carbonates  
84 from the Chobeni Formation (Nsuze Group, S. Africa). See Figure 1 and Data Repository  
85 for descriptions and locations of each unit and sample. Major element concentrations  
86 were measured on a HORIBA Ultima 2 ICP-AES after HF-HNO<sub>3</sub> total digestion, trace  
87 elements on carbonate leaches (5% acetic acid) using a ThermoFisher Scientific  
88 Element2 HR-ICP-MS, and Mo isotopic compositions on a ThermoFisher Scientific  
89 Neptune MC-ICP-MS after 6N HCl digestion, double spike (DS, <sup>97</sup>Mo<sup>100</sup>Mo) addition,  
90 and chromatographic purification of Mo. Mo concentrations were calculated by isotope  
91 dilution. All analyses were performed at the Pôle Spectrometry Ocean, Brest, France. For  
92 all data (new and compiled), δ<sup>98</sup>Mo values are reported relative to the NIST3134 standard  
93 set to 0.25‰ (Nägler et al., 2014; see Table DR1 for details), uncertainties are reported as  
94 two standard deviations (2SD), and datasets are tabulated in Tables DR2 to DR6. See  
95 Data Repository for extended methods.

96

97 **RESULTS AND DISCUSSION**

98 **The Phanerozoic Mo Isotope Record**

99 The modern seawater  $\delta^{98}\text{Mo}$  value of 2.36‰ ( $\pm 0.1\%$ , Siebert et al., 2003) is  
100 reflected in the maximal  $\delta^{98}\text{Mo}$  values of both modern black shales and carbonates (See  
101 Figure 2A, Tables DR3 and DR4). With a maximum value of 1.76‰, our new data from  
102 modern Bahamian microbialites fall within the range observed for contemporaneous  
103 carbonates, but due to detrital impurities, or local production of sulfide, they do not reach  
104 the modern seawater value (see sample description in the DR; Figure 2A and Table  
105 DR2). For all available carbonate data,  $\delta^{98}\text{Mo}$  values are never heavier than modern  
106 seawater and are thus useful for constraining the minimum value of seawater at any given  
107 time (Figure 2A).

108 During the Phanerozoic, carbonates record a range of  $\delta^{98}\text{Mo}$  values from 2.42‰  
109 to -0.91‰ (see Figure 2A), with maximum values universally attaining the modern  
110 seawater value of  $2.36 \pm 0.1\%$  (Figure 2A). Shales record a range of  $\delta^{98}\text{Mo}$  values similar  
111 to carbonates (from 2.44‰ to -1‰), but also include the few outliers lower than -1‰.  
112 Only about one-fifth of compiled Phanerozoic shale values fall within 1‰ of the modern  
113 seawater value, in part due to non-quantitative Mo removal. Carbonates are also limited  
114 in their ability to record seawater signatures, notably by their low Mo contents that make  
115 them susceptible to diagenetic resetting or dilution by detrital materials, by the presence  
116 of organic matter or porewater sulfide during diagenesis that may alter whole-rock  
117 values, and/or their pervasive re-crystallization at even low metamorphic grades.  
118 Nonetheless, carbonates provide complimentary insight into Mo cycling during periods  
119 when shale records fall short.

120

121 **Mo Cycling in the Precambrian**

122 For the Proterozoic, no Mo isotope data are available for carbonate rocks.  
123 Maximum values for shales are highly variable, ranging from -0.09‰ to 1.98‰ and  
124 averaging  $0.81 \pm 1.31$ ‰; Arnold et al. (2004) inferred a Proterozoic  $\delta^{98}\text{Mo}_{\text{sw}}$  value of  
125 1.08‰. Available IF data during this period are limited, but universally heavy in  $\delta^{98}\text{Mo}$ ,  
126 with maximum values for each deposit ranging from 1.03‰ to 2.08‰ (n=3). Archean  
127 Mo isotope data are more abundant in literature for all three lithologies, and a significant  
128 contrast in Mo isotope compositions between the three lithologies appears to occur prior  
129 to ~2.6 Ga. Maximum shale values range from 1.72‰ to 1.76‰ and average  
130  $1.73 \pm 0.05$ ‰ from 2.50 Ga to 2.60 Ga, yet are universally low (ranging from -0.46‰ to  
131 0.89‰, averaging  $0.31 \pm 0.52$ ‰) before 2.64 Ga. In contrast, and with the exception of the  
132 Chobeni carbonates, maximum values for carbonates and IF are consistently positive  
133 from 2.50 Ga to 2.97 Ga (0.82‰ to 1.97‰ with an average of  $1.31 \pm 0.72$ ‰ for  
134 carbonates; 0.97‰ to 1.87‰ with an average of  $1.52 \pm 0.79$ ‰ for IF; see Figure 2B). As  
135 discussed below, this contrast likely relates to the chemical conditions that enable the  
136 capture of seawater molybdenum in shale records.

137 From 2.50 to 2.60 Ga, maximum  $\delta^{98}\text{Mo}$  values in shales and carbonates vary from  
138 1.40‰ to 1.97‰, and their average places a lower limit on global seawater Mo isotopic  
139 composition of  $1.63 \pm 0.48$ ‰ during this period (Figure 2B). IF deposits analyzed during  
140 this period present a maximum value between 0.97‰ and 1.76‰. New data from 2.52 Ga  
141 carbonate samples from the Gamohaam Formation, Griqualand West basin, show a  
142 maximum  $\delta^{98}\text{Mo}$  of 1.11‰, in line with elevated values observed for carbonates of the

143 adjacent Transvaal basin (up to 1.97‰; Eroglu et al., 2015; Figure 2B). The general  
144 agreement in maximum  $\delta^{98}\text{Mo}$  values for available shale, carbonate, and IF records  
145 during this period is remarkable. All three archives appear to record seawater that is  
146 isotopically heavy due to sequestration of light Mo isotopes by Mn(IV)- and Fe(III)-oxide  
147 exit channels, consistent with evidence for increasing surface redox potential in the run-  
148 up to the GOE. Enhanced supply of sulfate (and likely Mo) to the oceans at this time and  
149 the development of euxinic conditions (e.g., Reinhard et al., 2009) would have promoted  
150 the authigenic enrichment of seawater Mo into organic-rich shales.

151 In several carbonate samples measured by others (Voegelin et al., 2010; Eroglu et  
152 al., 2015),  $\delta^{98}\text{Mo}$  compositions are isotopically light (as low as -0.82‰), indicating the  
153 former presence of Mn(IV)- or Fe(III)-oxides in the samples. As chemical sediments that  
154 often contain little detrital material, Precambrian carbonates are generally characterized  
155 by low Mo concentrations (<200 ppb), with average isotope-dilution whole rock Mo  
156 concentrations of  $140 \pm 470$  ppb for the period 2.50 to 2.97 Ga (Voegelin et al., 2010;  
157 Eroglu et al., 2015; this study). By contrast, shales generally reflect crustal Mo  
158 abundances (1.1 ppm; Rudnick and Gao, 2003), unless authigenic enrichment from  
159 seawater occurs. Accordingly, detritus-poor carbonate rocks should be more sensitive to  
160 the addition of small amounts of isotopically light Mo associated with Mn(IV)- or  
161 Fe(III)-oxide sedimentary inputs.

162 Our dataset includes the first available Mo isotope data for carbonates older than  
163 2.64 Ga. Microbialitic calcite and aragonitic crystal fans (now replaced by calcite) from  
164 the 2.80 Ga Mosher Formation at Steep Rock (Canada) show a maximum  $\delta^{98}\text{Mo}$  value of  
165  $1.22 \pm 0.04$ ‰, comparable to dolomitic stromatolites and dolomitized crystal fans from the

166 2.93 Ga Ball Assemblage at Red Lake (Canada) that display a maximum  $\delta^{98}\text{Mo}$  value of  
167  $1.03\pm 0.03\%$  (Figure 2B). Both of these values are remarkably heavy. While the low Mo  
168 contents of these samples might make their  $\delta^{98}\text{Mo}$  values more susceptible to diagenetic  
169 alteration, multiple lines of evidence indicate this was not responsible for heavy isotope  
170 enrichments prior to 2.64 Ga. Briefly, there is no relationship between  $\delta^{98}\text{Mo}$  and  
171  $\delta^{18}\text{O}_{\text{carb}}$ , and  $\delta^{98}\text{Mo}$  data tend toward crustal values as a function of degree of  
172 silicification (see discussion in Data Repository and Figures DR4 and DR5).  
173 Furthermore, burial of light Mo with organic carbon at concentrations typical of Archean  
174 shale is unlikely to have affected the global marine Mo cycle (see Data Repository).  
175 Instead, these heavy values suggest that Mn(IV)- and Fe(III)-oxide exit channels for Mo  
176 were sufficiently important to impart a heavy Mo isotope signature on Mesoarchean  
177 seawater. This conclusion is similar to that of Planavsky et al. (2014) and Ossa Ossa et al.  
178 (2018), who also concluded that an Mn(IV)-oxide exit channel was in operation ca. 2.95  
179 Ga. Crucially, the isotopically light data of these studies simply implies some unknown  
180 degree of Mo removal by an oxide-based exit channel, while the isotopically heavy data  
181 in our new dataset (also present in the IF examined by Planavsky et al., 2014) reflects the  
182 composition of residual seawater.

183         If both carbonates (this study) and iron formations (Planavsky et al., 2014) are  
184 characterized by Mo isotope compositions reflecting an important role for metal oxide-  
185 based Mo sinks prior to 2.7 Ga, then with the exception of recently analyzed shales from  
186 the Pongola Supergroup (Ossa Ossa et al., 2018), why has this not been detected in the  
187 larger shale record? Several possible explanations for this discrepancy exist, notably the  
188 possibility of spatial heterogeneity in seawater  $\delta^{98}\text{Mo}$  (see below and supplementary

189 discussion). However, considering that nearly all available data for shales older than 2.64  
190 Ga show  $\delta^{98}\text{Mo}$  values in the crustal range, we suggest that the most parsimonious  
191 explanation is that most shales simply did not experience authigenic Mo enrichment prior  
192 to 2.64 Ga. Indeed, shales older than  $\sim 2.64$  Ga rarely show signs of enrichment in Mo  
193 above crustal values (Figure 2B) and generally reflect detrital Mo sources. This can be  
194 explained by the fact that euxinic conditions that strongly promote Mo enrichment in  
195 shales were generally absent, whereas after 2.63 Ga, when the first euxinic conditions  
196 were established (e.g., Reinhard et al., 2009), carbonates and shales show comparable  
197  $\delta^{98}\text{Mo}$  records. Moreover, shales deposited under anoxic but non-euxinic conditions  
198 today still become authigenically enriched in Mo; it would appear that lower marine Mo  
199 concentrations rendered this process less effective in the Archean. In this context,  
200 carbonates that contain a smaller Mo contribution from detrital components, and do not  
201 depend on local euxinia or a large marine Mo reservoir for authigenic enrichment,  
202 provide unique insight into the upper limit of  $\delta^{98}\text{Mo}$  evolution of seawater prior to 2.63  
203 Ga that is otherwise cryptic in the shale sedimentary record. The rare cases where  
204 authigenic signals are recorded in shales (e.g., Ossa Ossa et al., 2018) point to the  
205 intriguing possibility of localized Mo isotope responses to local redox conditions.

206         The new carbonate  $\delta^{98}\text{Mo}$  data presented here show no relation with Mn content  
207 or Mn/Fe ratio, and considered in light of other redox indicators such as the presence of  
208 negative Ce anomalies (represented here as  $\text{Pr}/\text{Pr}^* > 1$ ; see Data Repository), it becomes  
209 apparent that interpretation of carbonate  $\delta^{98}\text{Mo}$  data may not always be straightforward.  
210 Simple mixing calculations reveal that the Mo isotope composition of carbonates is more  
211 resistant to dilution by detrital material than REE-based signatures (Figure 3). However,

212 paired  $\delta^{98}\text{Mo}$  – Ce anomaly data from the 2.97 Ga Chobeni Formation (Figure 3) reveal  
213 the presence of significant negative Ce anomalies, as reported elsewhere (Siahi et al.,  
214 2018), yet show no sign of Mo isotope fractionation outside of the crustal range. This  
215 apparent contradiction may be reconciled by the significantly shorter residence times of  
216 light REE (<300 years; see Data Repository) compared to Mo (likely greater than 17 ky  
217 during the Archean; Asael et al., 2015), making REE signals a local proxy, and as a  
218 result, the two proxies are necessarily recording redox at different spatial and temporal  
219 scales. Thus, one interpretation of the paired Chobeni  $\delta^{98}\text{Mo}$ -Ce anomaly data is that the  
220 basin experienced oxidative Ce cycling at a local scale, while oxic sinks for Mo remained  
221 minor in seawater at a global scale. The reverse is true for Red Lake samples, while the  
222 Mosher carbonate shows evidence for both local Mn(IV) oxide precipitation (positive  
223 Pr/Pr\*, consistent with Riding et al., 2014, Fralick and Riding, 2015) as well as global  
224 Mn(IV) oxide precipitation (positive  $\delta^{98}\text{Mo}$ ). For the Chobeni, another possibility is that  
225 mixing occurred between authigenic Mo from seawater and oxide sources, with the  
226 resulting mixture falling within the crustal  $\delta^{98}\text{Mo}$  range. Some points fall below the  
227 crustal  $\delta^{98}\text{Mo}$  range, supporting this possibility. While caution is warranted as late  
228 oxidative alteration of surface samples may be difficult to detect (Albut et al., 2018), our  
229 Chobeni dataset is consistent with at least some O<sub>2</sub> present locally in the basin, similar to  
230 recent findings based on REE data (Siahi et al., 2018) and Fe, Mo and S isotope data  
231 (Eickmann et al., 2018; Ossa Ossa et al., 2018).

232

233 **CONCLUSION**

234 This study presents the first  $\delta^{98}\text{Mo}$  data for carbonates older than 2.64 Ga, with  
235 values ranging from -1.54‰ to 1.22‰. By contrast, Mo isotope compositions of shales of  
236 similar age generally show crustal values. We suggest that this discrepancy results from  
237 low concentrations of Mo in seawater as well as a general absence of euxinic conditions.  
238 This, in turn, prevented widespread authigenic Mo enrichment in shales prior to the onset  
239 of oxidative continental weathering, an increased Mo reservoir, and the first  
240 establishment of localized euxinia ca. 2.7–2.6 Ga (e.g., Reinhard et al., 2009). Carbonate  
241 rocks are not subject to these constraints, and along with IF, provide additional  
242 perspective on the  $\delta^{98}\text{Mo}$  composition of Mesoarchean seawater. Our dataset further  
243 indicates minimum global seawater  $\delta^{98}\text{Mo}$  values of 1.2‰ and 1.0‰ at 2.80 and 2.93 Ga,  
244 respectively, consistent with the idea that Mn(IV)- and Fe(III)- oxide sinks for Mo were  
245 globally important as far back as 2.95 Ga (Planavsky et al., 2014; Ossa Ossa et al, 2018).  
246 Despite possible limitations stemming from detrital contamination and mixing of  
247 different authigenic components in the same sample, the  $\delta^{98}\text{Mo}$  composition of  
248 carbonates is a promising proxy for understanding marine molybdenum cycling and  
249 paleoredox evolution before conditions permitted widespread authigenic Mo enrichment  
250 in shales.

251

## 252 REFERENCES CITED

253 Albut, G., Babechuk, M. G., Kleinhanns, I. C., Bengner, M., Beukes, N. J., Steinhilber, B.,  
254 Smith, A. J. B., Kruger, S. J., Schoenberg, R., 2018, Modern rather than  
255 Mesoarchean oxidative weathering responsible for the heavy stable Cr isotopic

- 256 signatures of the 2.95 Ga old Ijzermijn iron formation (South Africa): *Geochimica et*  
257 *Cosmochimica Acta*, v. 228, p. 157-189, doi: 10.1016/j.gca.2018.02.034.
- 258 Arnold, G. L., Anbar, A., Barling, J., and Lyons, T., 2004, Molybdenum isotope evidence  
259 for widespread anoxia in mid-Proterozoic oceans: *Science*, v. 304, p. 87–90, doi:  
260 10.1126/science.1091785.
- 261 Asael, D., Rouxel, O., Bekker, A., and Scott, C., 2015, Dissolved Mo in the Archean  
262 oceans - a case study from the 2.63 Ga Jeerinah Formation, Australia: *Goldschmidt*,  
263 25th, p. 121.
- 264 Barling, J., and Anbar, A. D., 2004, Molybdenum isotope fractionation during adsorption  
265 by manganese oxides: *Earth and Planetary Science Letters*, v. 217, p. 315-329, doi:  
266 10.1016/S0012-821X(03)00608-3.
- 267 Eickmann, B., Hofmann, A., Wille, M., Bui, T. H., Wing, B. A., and Schoenberg, R.,  
268 2018, Isotopic evidence for oxygenated Mesoarchean shallow oceans: *Nature*  
269 *Geoscience*, p.1, doi: 10.1038/s41561-017-0036-x.
- 270 Eroglu, S., Schoenberg, R., Wille, M., Beukes, N., and Taubald, H., 2015, Geochemical  
271 stratigraphy, sedimentology, and Mo isotope systematics of the ca. 2.58–2.50 Ga-old  
272 Transvaal Supergroup carbonate platform, South Africa: *Precambrian Research*, v.  
273 266, p. 27–46, doi: 10.1016/j.precamres.2015.04.014.
- 274 Goldberg, T., Archer, C., Vance, D., and Poulton, S. W., 2009, Mo isotope fractionation  
275 during adsorption to Fe (oxyhydr) oxides: *Geochimica et Cosmochimica Acta*, v. 73,  
276 p. 6502–6516, doi: 10.1016/j.gca.2009.08.004.
- 277 Nägler, T. F., Anbar, A. D., Archer, C., Goldberg, T., Gordon, G. W., Greber, N. D.,  
278 Siebert, C., Sohrin, Y., and Vance, D., 2014, Proposal for an International

- 279 Molybdenum Isotope Measurement Standard and Data Representation: *Geostandards*  
280 and *Geoanalytical Research*, v. 38, p. 149-151, doi: 10.1111/j.1751-  
281 908X.2013.00275.x.
- 282 Neubert, N., Nägler, T. F., and Böttcher, M. E., 2008, Sulfidity controls molybdenum  
283 isotope fractionation into euxinic sediments: Evidence from the modern Black Sea:  
284 *Geology*, v.36, p. 775–778, doi: 10.1130/G24959A.1.
- 285 Ossa Ossa, F., Hofmann, A., Wille, M., Spangenberg, J. E., Bekker, A., Poulton, S. W.,  
286 Eickmann, B., Schoenberg, R., 2018, Aerobic iron and manganese cycling in a  
287 redox-stratified Mesoarchean epicontinental sea: *Earth and planetary science letters*,  
288 v. 500, p. 28-40, doi: 10.1016/j.epsl.2018.07.044.
- 289 Planavsky, N. J., et al., 2014, Evidence for oxygenic photosynthesis half a billion years  
290 before the Great Oxidation Event: *Nature Geoscience*, v. 7, p. 283, doi:  
291 10.1038/NGEO2122.
- 292 Reinhard, C. T., Raiswell, R., Scott, C., Anbar, A. D., and Lyons, T. W., 2009, A late  
293 Archean sulfidic sea stimulated by early oxidative weathering of the continents:  
294 *Science*, v. 326, p. 713–716, doi: 10.1126/science.1176711.
- 295 Riding, R., Fralick, P., and Liang, L., 2014, Identification of an Archean marine oxygen  
296 oasis: *Precambrian Research*, v. 251, p. 232–237, doi:  
297 10.1016/j.precamres.2014.06.017.
- 298 Fralick, P.W. and Riding, R., 2015, Steep Rock Lake: Sedimentology and geochemistry  
299 of an Archean carbonate platform: *Earth-Science Reviews*, v. 151, p. 132-175, doi:  
300 Fralick, P., & Riding, R. (2015). Steep Rock Lake: Sedimentology and geochemistry

- 301 of an Archean carbonate platform. *Earth-Science Reviews*, 151, 132–175.  
302 doi:10.1016/j.earscirev.2015.10.006.
- 303 Romaniello, S. J., Herrmann, A. D., and Anbar, A. D., 2016, Syndepositional diagenetic  
304 control of molybdenum isotope variations in carbonate sediments from the Bahamas:  
305 *Chemical Geology*, v. 438, p. 84–90, doi: 10.1016/j.chemgeo.2016.05.019.
- 306 Rudnick, R. L., and Gao, S., 2003, *Composition of the continental crust: Treatise on*  
307 *geochemistry*, v. 3, p. 659, doi: 10.1016/B0-08-043751-6/03016-4.
- 308 Siah, M., Hofmann, A., Master, S., Wilson, A., and Mayr, C., 2018, Trace element and  
309 stable (C, O) and radiogenic (Sr) isotope geochemistry of stromatolitic carbonate  
310 rocks of the Mesoproterozoic Pongola Supergroup: Implications for seawater  
311 composition: *Chemical Geology* v. 476, p. 389–406, doi:  
312 10.1016/j.chemgeo.2017.11.036.
- 313 Siebert, C., Nägler, T. F., von Blanckenburg, F., and Kramers, J. D., 2003, Molybdenum  
314 isotope records as a potential new proxy for paleoceanography: *Earth and Planetary*  
315 *Science Letters*, v. 211, p. 159–171, doi: 10.1016/S0012-821X(03)00189-4.
- 316 Siebert, C., Kramers, J., Meisel, T., Morel, P., and Nägler, T. F., 2005, PGE, Re-Os, and  
317 Mo isotope systematics in Archean and early Proterozoic sedimentary systems as  
318 proxies for redox conditions of the early Earth: *Geochimica et Cosmochimica Acta*,  
319 v. 69, p. 1787–1801, doi: 10.1016/j.gca.2004.10.006.
- 320 Voegelin, A. R., Nägler, T. F., Samankassou, E., and Villa, I. M., 2009, Molybdenum  
321 isotopic composition of modern and carboniferous carbonates: *Chemical Geology*, v.  
322 265, p. 488–498, doi: 10.1016/j.chemgeo.2009.05.015.

- 323 Voegelin, A. R., Nägler, T. F., Beukes, N. J., and Lacassie, J. P., 2010, Molybdenum  
324 isotopes in late Archean carbonate rocks: implications for early Earth oxygenation:  
325 Precambrian Research, v. 182, p. 70–82, doi: 10.1016/j.precamres.2010.07.001.
- 326 Voegelin, A. R., Nägler, T. F., Pettke, T., Neubert, N., Steinmann, M., Pourret, O., and  
327 Villa, I. M., 2012, The impact of igneous bedrock weathering on the Mo isotopic  
328 composition of stream waters: Natural samples and laboratory experiments:  
329 Geochimica et Cosmochimica Acta, v. 86, p. 150–165, doi:  
330 10.1016/j.gca.2012.02.029.
- 331 Wen, H., Carignan, J., Zhang, Y., Fan, H., Cloquet, C., and Liu, S., 2011, Molybdenum  
332 isotopic records across the Precambrian-Cambrian boundary: Geology, v. 39, p. 775–  
333 778, doi: 10.1130/G32055.1.
- 334 Wille, M., Kramers, J. D., Nägler, T. F., Beukes, N., Schröder, S., Meisel, T., Lacassie,  
335 J., and Voegelin, A., 2007, Evidence for a gradual rise of oxygen between 2.6 and  
336 2.5 Ga from Mo isotopes and Re-PGE signatures in shales: Geochimica et  
337 Cosmochimica Acta, v. 71, p. 2417–2435, doi: 10.1016/j.gca.2007.02.019.

338

### 339 **Acknowledgments**

340 We thank Dawn Sumner for providing samples and Olivier Rouxel for providing  
341 Mo standards and double spike. We also thank Emmanuel Ponzevera, Alexis de Prunelé,  
342 Yoan Germain, Bleuenn Guegen, Marie-Laure Rouget, and Céline Liorzou for analytical  
343 assistance, and Matthieu Plasman for GIS assistance. This work was supported by an  
344 NSERC Discovery Grant to K.O.K. (RGPIN-165831), an NSERC Discovery Grant to  
345 P.W.F. (RGPIN 16400), and an NSF EAR Grant to P.T.V (1561173). W.A.

346 acknowledges financial support by the Exxaro Chair at the University of Pretoria and by  
347 NRF Incentive Funding. S.V.L. acknowledges support from the European Union's  
348 Horizon 2020 research and innovation programme (grant agreement n° 716515). Ronny  
349 Schönberg and two anonymous reviewers are thanked for their constructive and  
350 insightful reviews.

351

352 **FIGURE CAPTIONS**

353 Figure 1. Maps showing (A) Canadian and (B) South African Archean carbonate  
354 occurrences analyzed in this study. See Data Repository for additional details and GPS  
355 coordinates.

356

357 Figure 2. New and compiled  $\delta^{98}\text{Mo}$  data for shales, iron formations, and carbonates  
358 through geological time: (A) data from 3.5 Ga to present; (B) focus on the period from  
359 2.5 Ga to 3.0 Ga. See Data Repository for values and data sources. The dark grey area  
360 represents modern continental crust values ( $\pm 2\text{SD}$ ; Siebert et al., 2003) and the light grey  
361 area represents the value of modern seawater ( $\pm 2\text{SD}$ ; Siebert et al., 2003). (C) New and  
362 compiled Mo concentration data for shales, iron formation, and carbonates through  
363 geological time.

364 Figure 3.  $\delta^{98}\text{Mo}$  data for carbonate samples analyzed in this study plotted against PAAS-  
365 normalized Pr anomalies as a proxy for true Ce anomalies (see Data Repository). Grey  
366 areas represent crustal ranges for both proxies, with the darker grey box indicating their  
367 intersection; black lines represent mixing trajectories between crust ( $\delta^{98}\text{Mo}\approx 0\text{‰}$  and  
368  $\text{Pr}/\text{Pr}^*=1$ ) and different authigenic end-members, including modern seawater  
369 ( $\delta^{98}\text{Mo}=2.36\text{‰}$  and  $\text{Pr}/\text{Pr}^*=1.4$ ) and different hypothetical  $\delta^{98}\text{Mo}$  compositions of  
370 ancient seawater and Mn- and Fe-oxides ( $\delta^{98}\text{Mo}$  ranging from 1.5 to  $0\text{‰}$ ;  $\text{Pr}/\text{Pr}^*$  fixed at  
371 1.2). Grey arrows show the trajectory of admixing of Mo associated with Mn- and Fe-  
372 oxide sources.

373

374 <sup>1</sup>GSA Data Repository item 2018xxx, containing supplemental discussion on marine Mo  
375 cycling and post-depositional modification, description of samples and their REE spectra,  
376 detailed methods and compilation data sources, and data tables, is available online at  
377 <http://www.geosociety.org/datarepository/2018/>, or on request from  
378 [editing@geosociety.org](mailto:editing@geosociety.org).

Figure 1

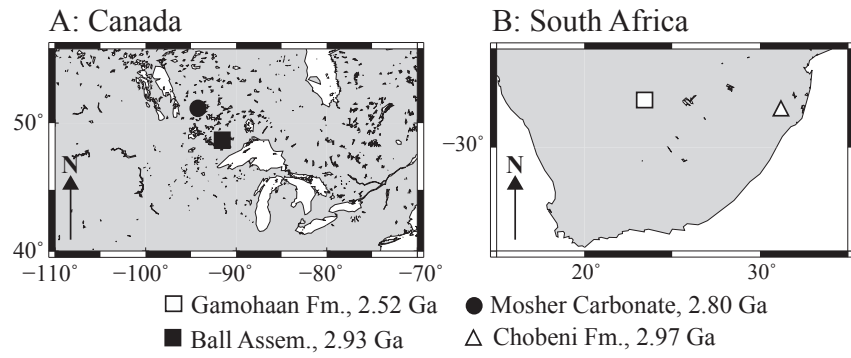


Figure 2

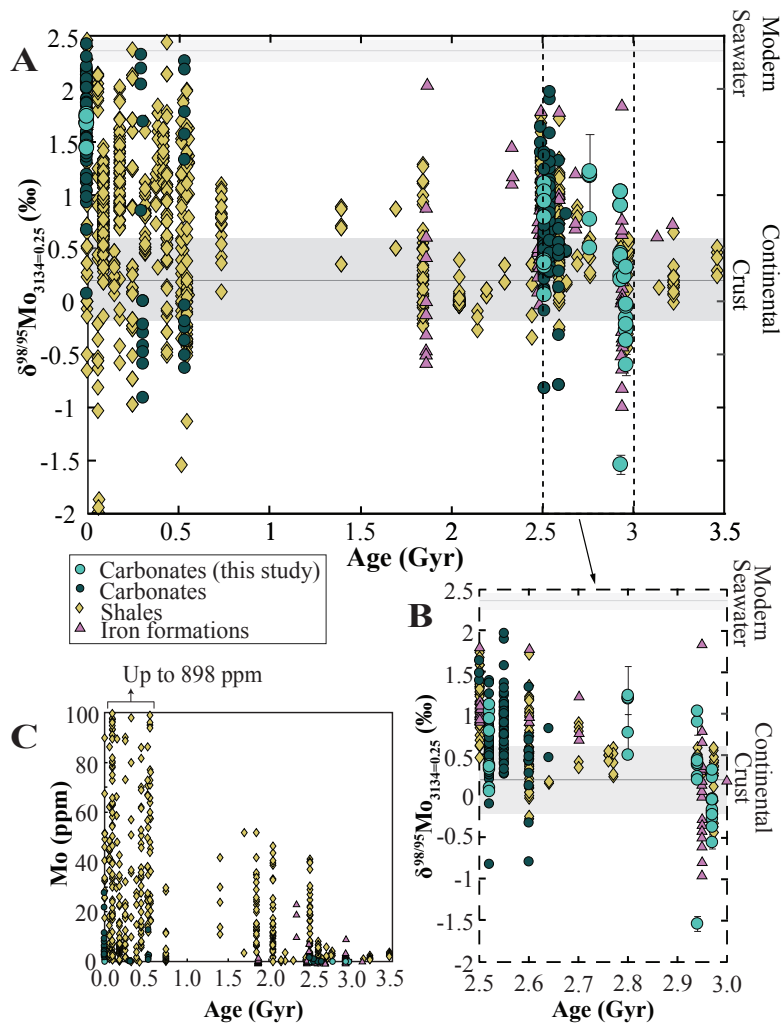


Figure 3

